MT-InSAR Optimisation for Structural Health Monitoring

Kuai, Hao; Macchiarulo, Valentina; Sharma, Satyadhrik; Karamitopoulos, Pantelis; Messali, Francesco; Giardina, Giorgia

DOI
10.58286/29753

Publication date
2024

Document Version
Final published version

Published in
e-Journal of Nondestructive Testing

Citation (APA)
Kuai, H., Macchiarulo, V., Sharma, S., Karamitopoulos, P., Messali, F., & Giardina, G. (2024). MT-InSAR Optimisation for Structural Health Monitoring. *e-Journal of Nondestructive Testing*. https://doi.org/10.58286/29753

eJNDT e-Journal of Nondestructive Testing - ISSN 1435-4934 - www.ndt.net

EWSHM 2024
11th European Workshop on Structural Health Monitoring

MT-InSAR Optimisation for Structural Health Monitoring

Hao KUAI [1,*], Valentina MACCHIARULO [1], Satyadhrik SHARMA [1], Pantelis KARAMITOPOULOS[1,2], Francesco MESSALI [1], Giorgia GIARDINA[1]
[1] Delft University of Technology, Stevinweg 1, Delft, 2628 CN, The Netherlands;
*h.kuai@tudelft.nl
[2]City of Amsterdam, Program of Bridges and Quay Walls, Team Innovation, Amsterdam, The Netherlands

Abstract. The implementation of effective and sustainable Structural Health Monitoring (SHM) systems for the evaluation of infrastructure conditions is critical to address the deterioration and damage experienced by structures worldwide. Given the vast number of structures involved, resorting to traditional in-situ visual inspections and data gathering methods is becoming increasingly unfeasible.

Multi-Temporal Interferometric Synthetic Aperture Radar (MT-InSAR) has recently gained attention as a viable solution for long-term SHM. This remote sensing technique combines multiple satellite radar images to measure changes in the Earth's surface over time. Unlike conventional techniques, MT-InSAR does not require in-situ installations and offers extensive coverage, enabling observations across diverse location and structures.

However, the applicability of MT-InSAR monitoring depends on the relatively unpredictable distribution and location of permanent scatterers (PSs), which are influenced by surface characteristics and vegetation changes. Evaluating the reliability and capacity of MT-InSAR is therefore crucial to enhance its effectiveness in assessing the location and extent of structural damage.

In this study, we present an effective approach to determine the optimal number and position of PSs for detecting different structural damage mechanisms. The approach is exemplified through a case study of a quay wall in Amsterdam, with data inputs simulated using the Finite Element Method. The proposed method has the potential to evaluate the feasibility of MT-InSAR for a broader range of scenarios, enabling to detect specific structural conditions.

Keywords: MT-InSAR, Structural Health Monitoring, Permanent Scatterers, Sensor Placement, Quay Walls

https://doi.org/10.58286/29753

1. Introduction

Civil infrastructures deteriorate over time due to ageing and environmental impacts, making Structural Health Monitoring (SHM) increasingly important, especially as structures age beyond their design life. Current damage detection approaches primarily rely on visual inspections and non-destructive tests [1, 2], which are costly, labour-intensive and offer limited coverage [3, 4]. Multi-Temporal Interferometric Synthetic Aperture Radar (MT-InSAR) offers a cost-effective, wide coverage alternative [5]. MT-InSAR processes a subset of pixels known as Permanent Scatterers (PSs), which exhibit stable backscattering characteristics over time [6]. The technique can achieve a millimetric accuracy [7] in displacement measurements, comparable to some conventional SHM methods.

Numerous studies have demonstrated the MT-InSAR's efficacy in detecting displacements and indicating damage conditions [8-10], with previous research primarily focusing on identifying abnormal displacements as a key method for structural damage detection [11]. However, PSs present uncertainties due to their unpredictable locations and distribution [5, 12]. The effectiveness of MT-InSAR as a SHM method hinges on its ability to accurately reconstruct a structure's entire displacement pattern from the available PSs. Since displacement patterns and their evolution differ across various damage scenarios, the key to MT-InSAR's utility in SHM lies in the adequacy of PSs to capture these patterns comprehensively.

To quantify such capability, this study aims to determine the necessary number and positions of PSs to fully and accurately reconstruct the displacement pattern corresponding to each damage scenario, using a structure-based inverse approach. Utilising displacement data, we retroactively identify optimal PSs locations, supported by a numerical model simulating the structure's damage progression. This model helps derive displacement data from damage onset to failure. By applying an Optimal PS Locations Selection (OPLS) algorithm, grounded in sparse sensor placement optimization principles [13], we aim to identify the optimal PS locations.

2. Methodology

The proposed structure-based inverse approach aims to determine the optimal PSs locations for a full detection of specific failure mechanisms, with the final objective of assessing MT-InSAR's capabilities for different structures and different load scenarios. Firstly, possible damage mechanisms are determined for the target structure. Then, the evolution of displacement patterns for these damage mechanisms are simulated numerically. Finally, the displacement patterns are processed to identify the optimal PSs locations via OPLS, ensuring comprehensive capture of the entire damage behaviour.

Possible Damage Mechanisms The first step consists in the identification of the potential damage mechanisms for the target, and the exclusion of those mechanisms that could not be detected by MT-InSAR monitoring. This filtering process is primarily guided by two criteria. Firstly, MT-InSAR can only detect surface movements of structures, and therefore any damage mechanisms that do not induce displacement on the surface of the structure should be disregarded. Secondly, considering the time intervals between each observation, MT-InSAR may fail to detect mechanisms characterized by very short duration from damage initiation to collapse.

Evolution of Displacement Patterns Through numerical simulations, displacement patterns from the previously selected mechanisms can be extracted at various steps of the progressive damage evolution. These displacement patterns serve as the basis for identifying the optimal PSs locations.

Optimal PSs Locations Selection (OPLS) Once the displacement patterns are obtained from numerical simulation, the optimal PSs locations can be determined using the OPLS method. The vector of PSs displacements can be described by:

$$\boldsymbol{y} = \boldsymbol{C}\boldsymbol{x} \tag{1}$$

where $\boldsymbol{C}$ represents the matrix of PSs locations and $\boldsymbol{x}$ is the complete displacement vector of the structure, which represents a specific damage mechanism at a given time. In general, it is in a high-dimensional state and can be represented sparsely using a basis $\boldsymbol{\Psi}$:

$$\boldsymbol{x} = \boldsymbol{\Psi}\boldsymbol{s} \tag{2}$$

where $\boldsymbol{s}$ is a sparse vector indicating the active modes in $\boldsymbol{\Psi}$.

The basis matrix $\boldsymbol{\Psi}$ in Equation 2 is generated from the numerical simulation. Each column of $\boldsymbol{\Psi}$ represents one structural point (a PS candidate), while each row corresponds to one time interval or load step during the damage evolution. Ideally $\boldsymbol{\Psi}$ contains all the information of one damage mechanism. No matter when MT-InSAR analysis is performed, we always can represent the MT-InSAR process as:

$$\boldsymbol{y} = \boldsymbol{C}\boldsymbol{x} = \boldsymbol{C}\boldsymbol{\Psi}\boldsymbol{s} \tag{3}$$

To reconstruct the displacement data for the entire structure, the primary step involves obtaining the sparse vector $\boldsymbol{s}$ using Moore-Penrose pseudoinverse [14]:

$$\boldsymbol{s} = (\boldsymbol{C}\boldsymbol{\Psi})^{\dagger}\boldsymbol{y} \tag{4}$$

In this case, optimizing PSs locations equates to obtaining an optimal matrix $\boldsymbol{C}$, ensuring minimal impact of disturbances in the detected displacement matrix $\boldsymbol{y}$, like noise, on $\boldsymbol{s}$ and, by extension, $\boldsymbol{x}$. This optimization problem can be re-framed as making the pseudoinverse $\boldsymbol{C}\boldsymbol{\Psi}$ as well-conditioned as possible.

There are several methods available for controlling the condition number of a matrix [15, 16]. In this research, we opted for a specialized Quadrature-based Discrete Empirical Interpolation Method known as pivoted QR factorization [17]. This choice is favoured due to its simplicity, cost-efficiency and wide-applicability.

For a potential damage mechanism, the pivoted QR factorization of a basis matrix $\boldsymbol{\Psi}$ produces three matrices: an orthonormal matrix $\boldsymbol{Q}$, an upper triangular matrix $\boldsymbol{R}$, and the measurement matrix $\boldsymbol{C}$ identified by the pivot column:

$$\boldsymbol{\Psi}^{\top}\boldsymbol{C}^{\top} = \boldsymbol{Q}\boldsymbol{R} \tag{5}$$

Pivots provided by QR factorization indicate the ranking of potential PSs. Determining the optimal number of PSs to capture the tested structure's behaviour often necessitates additional steps. As mentioned, the primary objective of MT-InSAR is to reconstruct the entire displacement pattern accurately. Therefore, the discrepancy between the reconstructed displacement pattern and the ideal pattern in the basis matrix or simulated in numerical modelling serves as a verification method for determining the necessary number of PSs. While various reconstruction methods exist, ranging from linear to nonlinear mapping techniques [18, 19], here we used the simplest approach, i.e. linear mapping, to test the overall approach effectiveness.

3. Case Study

The proposed methodology was implemented to determine optimal PSs location for a historic quay wall, located on Marnixkade, representative of the ones situated in the city centre of Amsterdam. The quay wall geometry is depicted in Fig. *1*. The commercial software Diana FEA was used for the numerical simulation [20]. Further details on the structure and the FE model are available from previous studies [21].

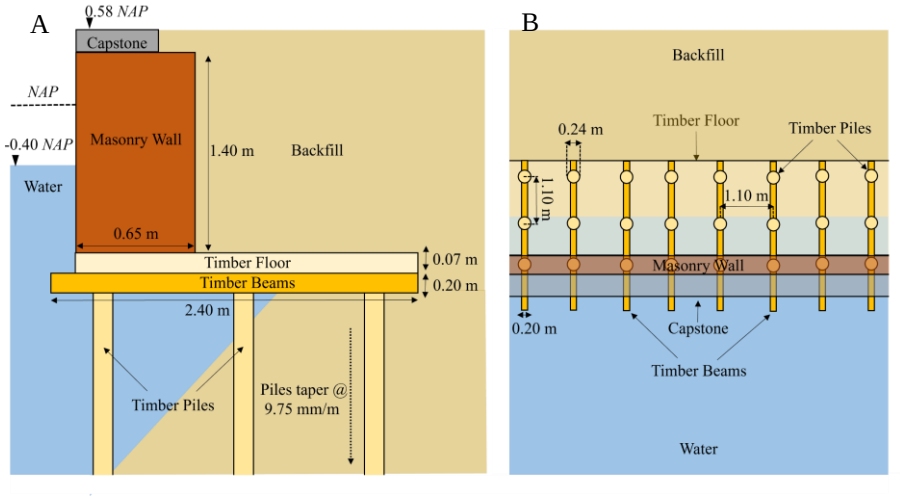

Fig. 1. Geometry of the Marnixkade quay wall [21]

(A) Transversal cross-section and (B) Plan view.

4. Analysis and Results

As an initial theoretical scenario, the analysed structure was tested by simulating the incremental application of lateral forces until failure. Such forces are obtained by considering the redistribution through the soil to the masonry wall and the adjacent timber floor of vertical loads corresponding to a truck located on the road next to the quay at a distance of 4 m. In addition to enabling a relatively straightforward tracking of displacement evolution, this load case scenario led to considerable displacements at the quay wall top surface, meeting the criteria for potential damage mechanisms detectable by MT-InSAR, as detailed in Section 2. Fig. *2* shows the displacement pattern of the quay wall at the end of the incremental load application.

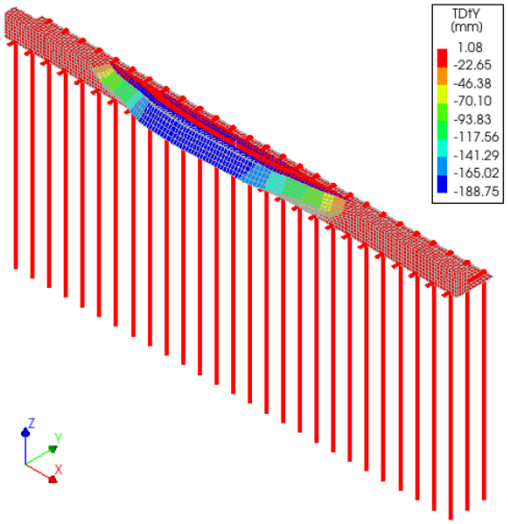

Fig. 2. Horizontal displacement and deformed configuration of the quay wall at the final load step (Displacement scale factor: 10)

The OPLS algorithm was applied to this displacement pattern. Following the ranking of nodes using pivoted QR factorization, we used the reconstruction error as a criterion for determining the required number of PSs, as outlined in Section 2. To ensure the accuracy of this determination, both the maximum absolute error and the mean square error, defined in terms of nodal displacements, were considered. The maximum absolute error was utilized to

quantify any abnormal deviations within the structure, while, the mean square error provided insight into the overall reconstruction behaviour, which is crucial. In total, the numerical model comprises 23,039 nodes, all of which serve as potential candidates for OPLS. In Fig. ***3***, the reconstruction errors have been successfully minimized to 0.002793 mm by selecting three PSs. This level of precision significantly exceeds the submillimetric accuracy of MT-InSAR [7].

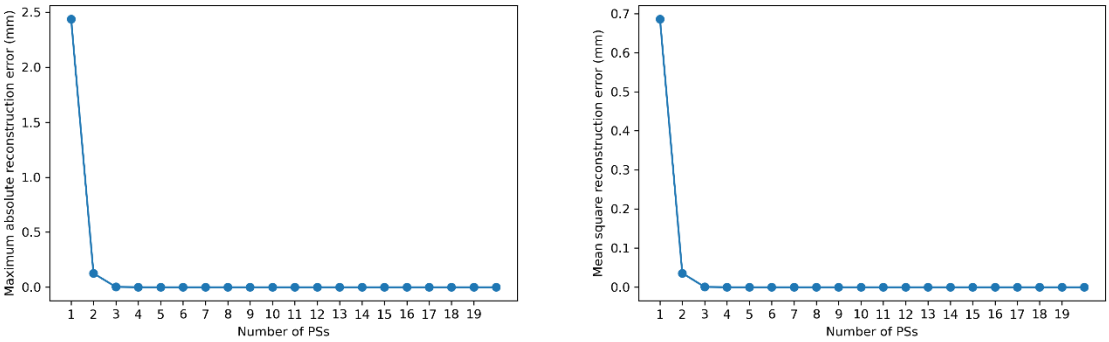

(a) Maximum absolute error (b) Mean square error

Fig. 3. Reconstruction error

The precise location of the three selected PSs is depicted in Fig. ***4***. The top-ranked PS is positioned at the centre of the quay wall, coinciding with the area exhibiting the largest displacement pattern. The second and third PSs are situated on either side of this central PS, somewhat near the boundary of the quay wall area experiencing significant displacement. This demonstrates that a limited number of available PSs can effectively identified broad failure patterns within a structure. The approach can be extended to different failure mechanisms and structural sections, moving beyond the limit of specific pinpoint locations, in this way accommodating the uncertainties associated with the precise positioning of PSs. The approach has therefore the potential to establish the minimal point requirements needed to reliably detect likely deterioration processes and failure mechanisms across different infrastructure assets.

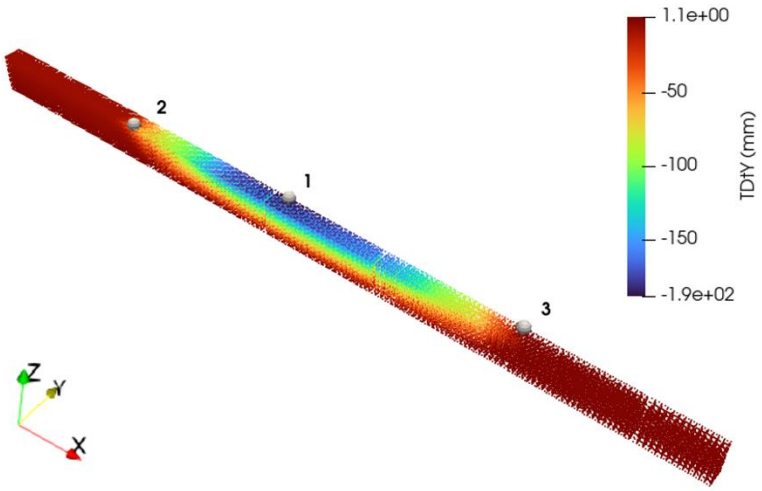

Fig. 4. Optimal PSs locations

5. Conclusion

In this paper we introduced a structural-based inverse approach to establish a benchmark for evaluating the efficacy of MT-InSAR in detecting structural failures. The method involves initially identifying which failure mechanisms can be detected by MT-InSAR. For these

detectable mechanisms, numerical models simulate the entire failure process, and a selected failure configuration is analysed using the OPLS algorithm to identify optimal PS locations. The approach is validated through the application of lateral loads to a quay wall FE model, indicating its potential future applicability to different structures and failure mechanisms.

Acknowledgments

This publication is part of the Vidi project InStruct, project number 18912, financed by the Dutch Research Council (NWO).

References

[1] Federal Highway Administration, "AASHTO - The Manual For Bridge Evaluation (3rd Edition, 2018)," Federal Highway Administration, FHWA-2017-0047-0274, May 2022. [Online]. Available: https://www.regulations.gov/document/FHWA-2017-0047-0274

[2] Higher Council of Public Works, "Guidelines for the Classification and Management of Risk, Safety Evaluation, and Monitoring of Existing Bridges," Ministry of Infrastructure and Transport, Jul. 2022. [Online]. Available: https://www.mit.gov.it/normativa/decreto-ministeriale-numero-204-del-1-luglio-2022

[3] P. Cawley, "Non-Destructive Testing—Current Capabilities and Future Directions," *Proc. Inst. Mech. Eng. Part J. Mater. Des. Appl.*, vol. 215, no. 4, pp. 213–223, Oct. 2001, doi: 10.1177/146442070121500403.

[4] J. Humar, A. Bagchi, and H. Xu, "Performance of Vibration-based Techniques for the Identification of Structural Damage," *Struct. Health Monit.*, vol. 5, no. 3, pp. 215–241, Sep. 2006, doi: 10.1177/1475921706067738.

[5] V. Macchiarulo, P. Milillo, C. Blenkinsopp, C. Reale, and G. Giardina, "Multi-Temporal InSAR for Transport Infrastructure Monitoring: Recent Trends and Challenges," *Proc. Inst. Civ. Eng. - Bridge Eng.*, vol. 176, no. 2, pp. 92–117, Jun. 2023, doi: 10.1680/jbren.21.00039.

[6] M. Crosetto, O. Monserrat, M. Cuevas-González, N. Devanthéry, and B. Crippa, "Persistent Scatterer Interferometry: A review," *ISPRS J. Photogramm. Remote Sens.*, vol. 115, pp. 78–89, May 2016, doi: 10.1016/j.isprsjprs.2015.10.011.

[7] A. Ferretti *et al.*, "Submillimeter Accuracy of InSAR Time Series: Experimental Validation," *IEEE Trans. Geosci. Remote Sens.*, vol. 45, no. 5, pp. 1142–1153, May 2007, doi: 10.1109/TGRS.2007.894440.

[8] V. Macchiarulo, P. Milillo, M. J. DeJong, J. González Martí, J. Sánchez, and G. Giardina, "Integrated InSAR Monitoring and Structural Assessment of Tunnelling-Induced Building Deformations," *Struct. Control Health Monit.*, vol. 28, no. 9, p. e2781, 2021, doi: 10.1002/stc.2781.

[9] P. Milillo, G. Giardina, D. Perissin, G. Milillo, A. Coletta, and C. Terranova, "Pre-Collapse Space Geodetic Observations of Critical Infrastructure: The Morandi Bridge, Genoa, Italy," *Remote Sens.*, vol. 11, no. 12, Art. no. 12, Jan. 2019, doi: 10.3390/rs11121403.

[10] S. Selvakumaran, S. Plank, C. Geiß, C. Rossi, and C. Middleton, "Remote monitoring to predict bridge scour failure using Interferometric Synthetic Aperture Radar (InSAR) stacking techniques," *Int. J. Appl. Earth Obs. Geoinformation*, vol. 73, pp. 463–470, Dec. 2018, doi: 10.1016/j.jag.2018.07.004.

[11] J. J. Sousa and L. Bastos, "Multi-temporal SAR interferometry reveals acceleration of bridge sinking before collapse," *Nat. Hazards Earth Syst. Sci.*, vol. 13, no. 3, pp. 659–667, Mar. 2013, doi: 10.5194/nhess-13-659-2013.

[12] R. F. Hanssen, "Satellite radar interferometry for deformation monitoring: a priori assessment of feasibility and accuracy," *Int. J. Appl. Earth Obs. Geoinformation*, vol. 6, no. 3, pp. 253–260, Mar. 2005, doi: 10.1016/j.jag.2004.10.004.

[13] K. Manohar, B. W. Brunton, J. Kutz, and S. Brunton, "Data-Driven Sparse Sensor Placement," *ArXiv*, Jan. 2017, Accessed: Mar. 14, 2024. [Online]. Available: https://www.semanticscholar.org/paper/Data-Driven-Sparse-Sensor-Placement-Manohar-Brunton/b589c3c24457aed7099bd07da865636dbe624a54

[14] R. Penrose, "A generalized inverse for matrices," *Math. Proc. Camb. Philos. Soc.*, vol. 51, no. 3, pp. 406–413, Jul. 1955, doi: 10.1017/S0305004100030401.

[15] S. Chaturantabut and D. C. Sorensen, "Nonlinear Model Reduction via Discrete Empirical Interpolation," *SIAM J. Sci. Comput.*, vol. 32, no. 5, pp. 2737–2764, Jan. 2010, doi: 10.1137/090766498.

[16] Z. Drmac and S. Gugercin, “A New Selection Operator for the Discrete Empirical Interpolation Method -- improved a priori error bound and extensions,” *SIAM J. Sci. Comput.*, vol. 38, no. 2, pp. A631–A648, Jan. 2016, doi: 10.1137/15M1019271.
[17] S. Ma, “Linear least squares solutions by Householder transformations with column pivoting on a parallel machine,” in *Proceedings High Performance Computing on the Information Superhighway. HPC Asia ’97*, Apr. 1997, pp. 134–136. doi: 10.1109/HPC.1997.592136.
[18] H. Wu, R. Dong, Z. Liu, H. Wang, and L. Liang, “Deformation Monitoring and Shape Reconstruction of Flexible Planer Structures Based on FBG,” *Micromachines*, vol. 13, no. 8, Art. no. 8, Aug. 2022, doi: 10.3390/mi13081237.
[19] A. Giannopoulos and J.-L. Aider, “Data-driven order reduction and velocity field reconstruction using neural networks: The case of a turbulent boundary layer,” *Phys. Fluids*, vol. 32, no. 9, p. 095117, Sep. 2020, doi: 10.1063/5.0015870.
[20] “DIANA FEA user’s manual - release, 10.5. Delft, Netherlands.” DIANA FEA B.V. Accessed: Mar. 29, 2024. [Online]. Available: https://dianafea.com/diana-manuals/
[21] S. Sharma, M. Longo, and F. Messali, “A novel tier-based numerical analysis procedure for the structural assessment of masonry quay walls under traffic loads,” *Front. Built Environ.*, vol. 9, 2023, Accessed: Feb. 15, 2024. [Online]. Available: https://www.frontiersin.org/articles/10.3389/fbuil.2023.1194658